Journal of Magnetism and Magnetic Materials 566 (2023) 170318

Contents lists available at ScienceDirect

Journal of Magnetism and Magnetic Materials

journal homepage: www.elsevier.com/locate/jmmm

Evidence for vortex state in Fe_2CoGe thin films using FORC and magnetic imaging

Rajesh Kumar Roul [a], Apu Kumar Jana [a], M. Manivel Raja [b], J. Arout Chelvane [b], S. Narayana Jammalamadaka [a,*]

[a] Magnetic Materials and Device Physics Laboratory, Department of Physics, Indian Institute of Technology Hyderabad, Hyderabad 502 284, India
[b] Defence Metallurgical Research Laboratory (DMRL), Hyderabad 500058, India

ARTICLE INFO

Keywords:
Vortex state
First order reversal curves
Magnetization reversal
Magnetic force microscope
MuMax^3

ABSTRACT

We report on the evidence for the vortex state in the thin films of Fe_2CoGe through first order reversal curves, magnetic force microscope, longitudinal magneto-optical Kerr effect and micro-magnetic simulations. Phase purity of the films confirmed through X-ray diffraction, which confirms the A2 type disorder Heusler alloy structure. Contour graph of first order reversal curves infers the formation of vortex state that is useful to understand magnetization reversal and switching process. We do observe the vortex state ~1 μm with in – plane curling of the magnetization using magnetic force microscope phase analysis. We believe that realization of vortex state formation in Fe_2CoGe thin films may cater applications in future magnetic data storage and microwave oscillators.

1. Introduction:

Magnetic vortices are topological excitations and are characterized by curling of in-plane magnetization, which allow one to explore fundamental nanoscale spin behaviour and also give an opportunity to utilize them in data storage technologies. These topological structures consist of a half-integer charge of $q = |wp/2| = 1/2$, where 'w' is winding number with the value of +1 and −1 for vortices and anti-vortices respectively. The polarity is the orientation of the core magnetization, either pointing up (p = 1) or down (p = −1). Simultaneously vortex also defined by a clockwise (c = 1) or counter-clockwise (c = −1) rotation of the in-plane magnetization. Magnetic vortices have attracted widespread interest in recent years, especially for their perspective applications in magnetic data storage [1–3] and microwave oscillators [4,5]. Indeed, the realization of magnetic vortex state has been quite challenging task and requires skilled experimentation. Among various experimental methods, first order reversal curves (FORC) have been identified to determine domain state configurations such as vortex and skyrmions [6–8]. Essentially, in this method, the magnetization can be de-convoluted for the reversible and irreversible parts that may give switching field distribution [9,10]. Recent study by Miguel A *"et al."* have shown vortex state in FORC contour graph for 64 nm Greigite (Fe_3S_4) particle [6]. In another study Chris Pike *"et al."* also have reported vortex nucleation and annihilation through FORC in submicron Co dots[11]. On the other hand, Ioan Lascu *"et al."* also have reported the signature of single vortex (SV) state in Geological material [12]. Apart from that, magnetic vortex states have been identified using magneto optical Kerr effect (MOKE) and magnetic force microscopy (MFM) phase analysis. Elena Pinilla-Cienfuegos, *"et al."* have reported the nucleation of vortex state with the tip stray field in $K_{0.22}Ni$ [Cr-$(CN)_6]_{0.74}$ nanopartiles [13]. On the other hand, Mironov *"et al."* also have reported magnetic vortex state in the their MFM phase images on Co nanodots [14]. Z. M. Dai *"et al."* have seen the nucleation and annihilation of the double-vortex and the single vortex states in [Co/Pd]$_7$/Ru/Py with applied magnetic field in their MOKE images [15]. In another study, Vavassori *"et al."* have reported the magnetization reversal of vortices in the elliptical disk with the in-plane applied field using MOKE imaging [16].

Among various magnetic alloy thin films, Heusler alloy thin films have been of great interest since they exhibit 100 % spin polarization at Fermi energy (E_F), which is critical for high tunnel magnetoresistance (TMR) values [17,18]. Heusler alloy compounds can be divided into two sub groups (a) half-Heusler alloys and (b) full-Heusler alloys. In the former, diagonally atoms are arranged like XYZ (X, Y are transition metal atoms and Z is sp atom like Al, Ge, Si *etc*) and consists C1b type structure, while X_2YZ is atomic arrangement along diagonal for the

* Corresponding author.
E-mail address: surya@phy.iith.ac.in (S. Narayana Jammalamadaka).

https://doi.org/10.1016/j.jmmm.2022.170318
Received 10 October 2022; Received in revised form 13 December 2022; Accepted 19 December 2022
Available online 21 December 2022

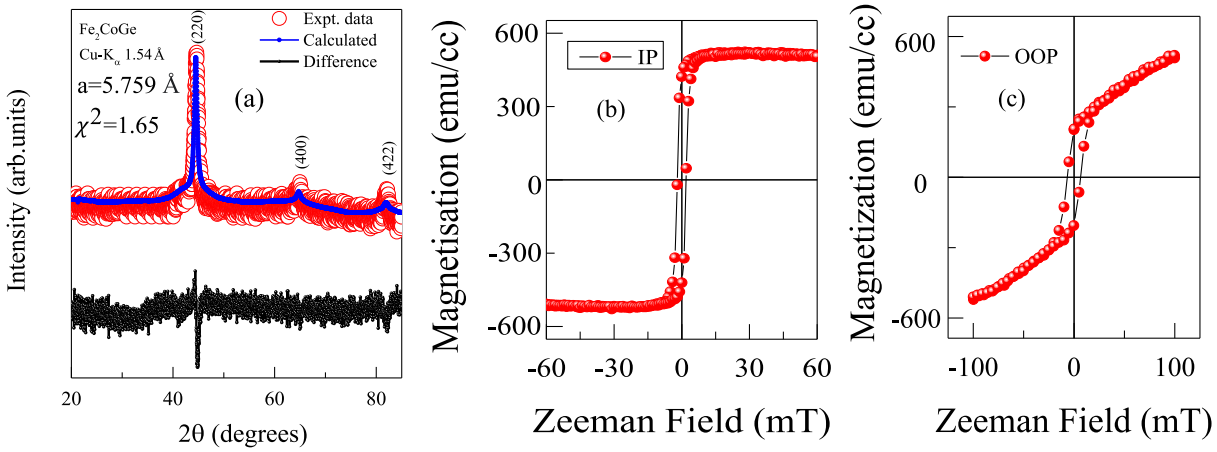

Fig. 1. **(a)** GI - XRD of Fe_2CoGe thin film. The diffraction patterns are fitted using FULL PROF software. Data with red circles infer experimental one, while blue line depicts the calculated data. Difference between them shown as black colour **(b)** Room temperature and in-plane magnetization (M) vs Zeeman field (H) of Fe_2CoGe thin films **(c)** Out of plane M vs H of Fe_2CoGe. (For interpretation of the references to colour in this figure legend, the reader is referred to the web version of this article.)

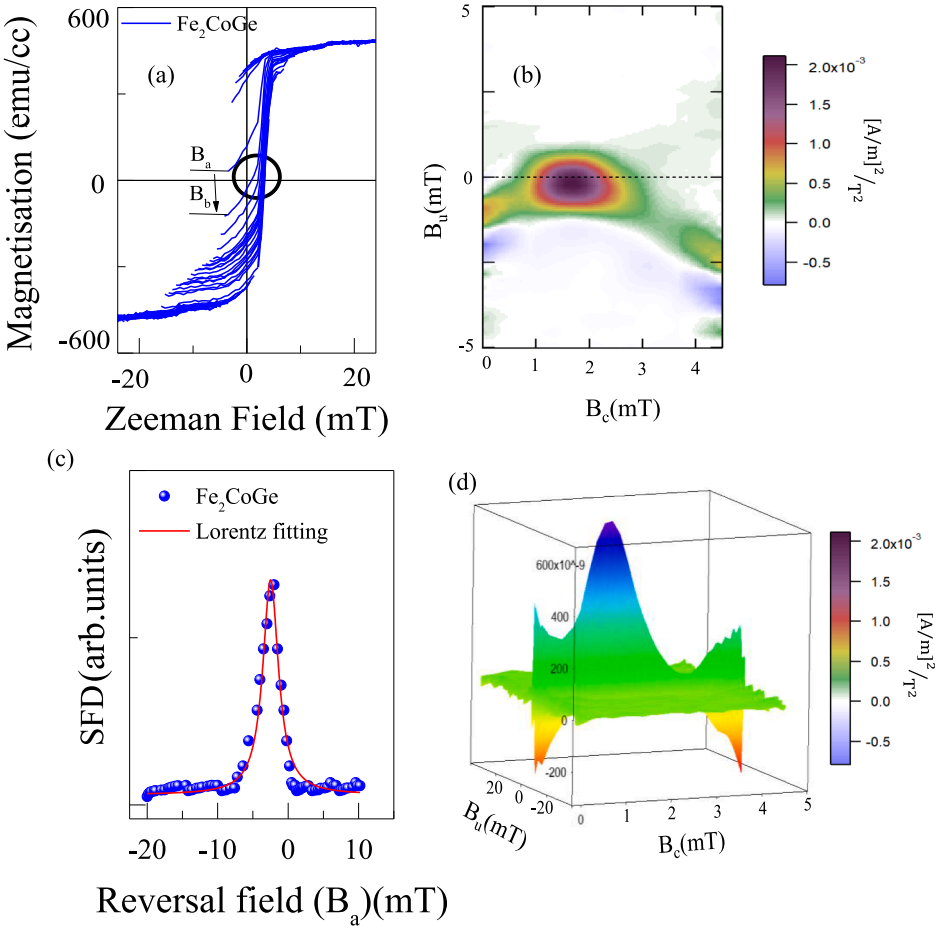

Fig. 2. **(a)** Magnetization vs Zeeman field graph for Fe_2CoGe thin films **(b)** FORC Contour graph **(c)** Switching field distribution (ρ) with Reversal field (B_a) **(d)** 3D plot of FORC distribution.

latter and form in $L2_1$ structure or B_2 or A_2 structures. In this work, we report on the nucleation of vortex state in Fe_2CoGe Heusler alloy thin films. This compound has been found to exhibit high magnetic moment (~5.3 μ_B), ferromagnetic Curie temperature at 700 K and high spin polarization ~ 70 % theoretically[19,20]. Determination and realization of domain state configuration in the thin films of Fe_2CoGe allow one to utilize these thin films for various spintronic applications such Giant magnetoresistance (GMR), Tunnelling Magnetoresistance (TMR) and spin valve devices. Salient features of present work are the realization of nucleation of vortex magnetic state in Fe_2CoGe thin film through (a) first order reversal curves (FORC) analysis (b) phase analysis of magnetic force microscopy (MFM) (c) magnetic domain imaging through

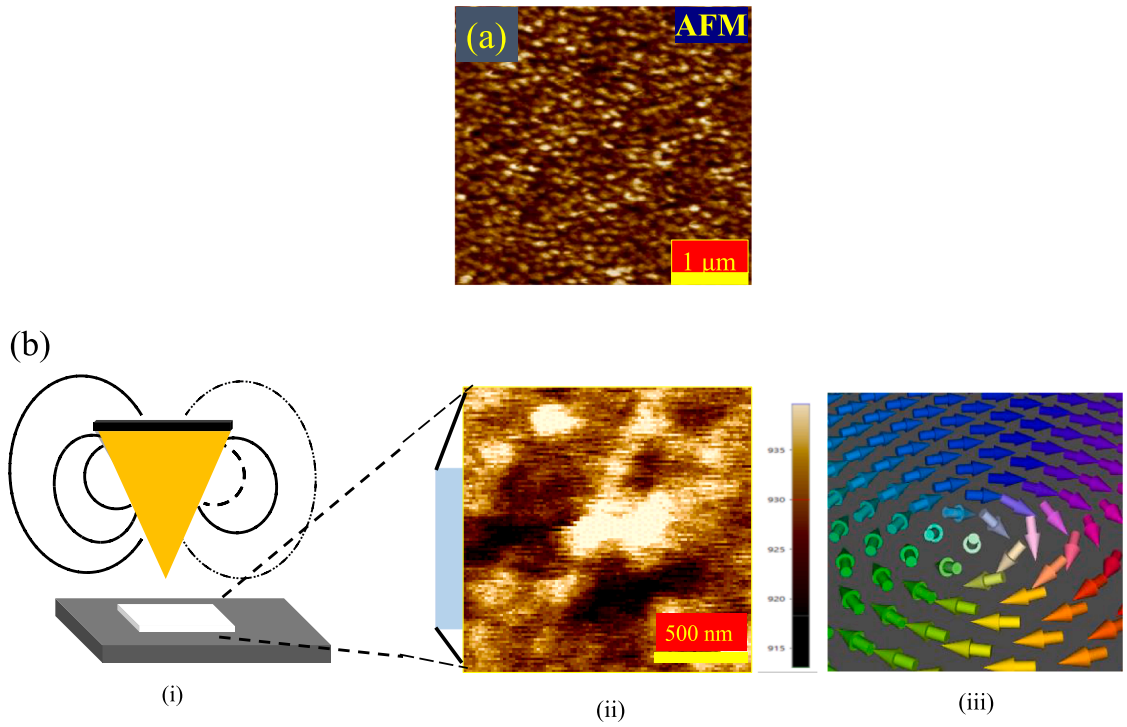

Fig. 3. (a) Surface morphology of Fe_2CoGe thin films through AFM imaging (b) (i) Schematic for the tip − sample relative position (ii) MFM phase image which reflects vortex state (iii) schematic of the spin structure pertinent to vortex state.

magneto-optic Kerr effect (MOKE) and (d) micromagnetic simulation using Landau–Lifshitz–Gilbert (LLG) equation.

2. Experimental

Initially, we prepared approximately 1 g of bulk polycrystalline Fe_2CoGe compound by conventional arc-melting using 99.99 % pure elements of Fe, Co and Ge respectively in an ultra-high purity argon atmosphere. The ingot was melted several times to get good homogeneity. The weight loss after final melting was 0.2 %. The prepared Fe_2CoGe ingot was broke into pieces for thermal evaporation to prepare thin film in ultra-high vacuum.

The pieces of Fe_2CoGe ingot were placed in tungsten boat for thermal evaporation (Advanced Processing Technologies (APT) make). The pressure of the chamber during the deposition was below 5×10^{-6} mbar and Silicon (Si) (1 0 0) was used as substrate. After deposition, phase purity of the Fe_2CoGe films were confirmed using the Rigaku Pro X-ray diffraction (XRD). Over here, we utilized the grazing incidence angle of $\theta = 0.5^{\circ}$ with Cu – k_α (1.54 Å) radiation at room temperature with a scan range of $2\theta = 20^{\circ} - 85^{\circ}$. The refinement of XRD data was performed using FULL PROF refinement software [21]. Surface morphology and magnetic phase information were obtained using Bruker Dimension ICON AFM/MFM. The CoCr coated antimony doped Si tips (MESP) were used for MFM imaging. First-order reversal curves measurement was performed using vibrating sample magnetometer (VSM) (Lakeshore 8607). The major hysteresis loops were measured in the magnetic field range of – 20 mT to 20 mT with a step size of 0.05 mT. For FORC data total of 130 loops were taken with an averaging time of 5 *sec* per each data point. A maximum magnetic field strength of 20 mT was applied to obtain a high-resolution FORC data. The raw data were analysed using FORCinel (V2.03 in IGOR PRO6, Wave metrics, Portland, OR) with a smoothing factor of 6 (SF = 6). Domain wall dynamics were studied using longitudinal magneto-optical Kerr effect (L – MOKE). Micromagnetic simulations were performed using Mumax3 software to support experimental data.

3. Results and discussion

Fig. 1(a) depicts the room temperature grazing incidence (GI) ($\theta = 0.5^{\circ}$) X – ray diffraction (XRD) pattern for Fe_2CoGe thin film. The GI-XRD pattern infer that the synthesized Fe_2CoGe thin film is in crystalline form with (2 2 0), (4 0 0) and (4 2 2) reflections and is consistent with the earlier reports by T. Gasi *"et al."* [19]. Essentially the existence of the above reflections infers A2 disorder type Heusler alloy structure with a space group of $Pm\overline{3}m$ in the absence of superstructure reflections such as (1 1 1) and (2 0 0) respectively. Further to confirm the structure and to determine lattice parameter, we have performed Rietveld refinement using FULL PROF software assuming the atomic position of individual elements pertinent to Fe_2CoGe Heusler alloy as Fe ($\frac{1}{4}, \frac{1}{4}, \frac{1}{4}$), Fe ($\frac{3}{4}, \frac{3}{4}, \frac{3}{4}$), Co ($\frac{1}{2}, \frac{1}{2}, \frac{1}{2}$) and Ge (0,0,0), which occupy the Wyckoff sites in the unit cell respectively [19,20,22]. Fig. 1 (a) shows the fitting of experimental XRD data using FULL PROF software. Red colour graph with circle symbol shows the experimental data, while blue line is fitted data. The difference is depicted as black colour graph at the bottom. The extracted lattice parameter after refinement is found to be 5.759 ± 0.002 Å, which is consistent with the previously reported value[19,20]. We do not see effect of fluorescence as we used diffracted beam monochromator (DBM) [23,24] while collecting XRD data.

The composition of the film is confirmed using energy dispersive X-ray spectroscopy (EDX) and is found to be in the ratio of 2:1:1. Further atomic force microscope (AFM) was used to determine surface roughness and the thickness of the film, which are found to be 1.26 nm and 110 nm respectively. During the film deposition, one edge of substrate is shadowed by Kapton tape. After the deposition, we removed the tape, which gave us step to measure thickness using AFM. Fig. 1 (b) and Fig. 1 (c) infer in-plane (IP) and out-of-plane (OPP) magnetization curves of Fe_2CoGe thin films. It is evident from Fig. 1 (b) that for in-plane measurements, magnetization saturated at 18 mT with $M_s \sim 527$ emu/cc and $H_c \sim 2$ mT respectively. On the other hand, we do not see saturation for out-of-plane magnetization ~ 100 mT as shown in Fig. 1 (c). From the above measurements, we confirm that our Fe_2CoGe thin film consists of in-plane magnetization. In order to elucidate the kind of domain

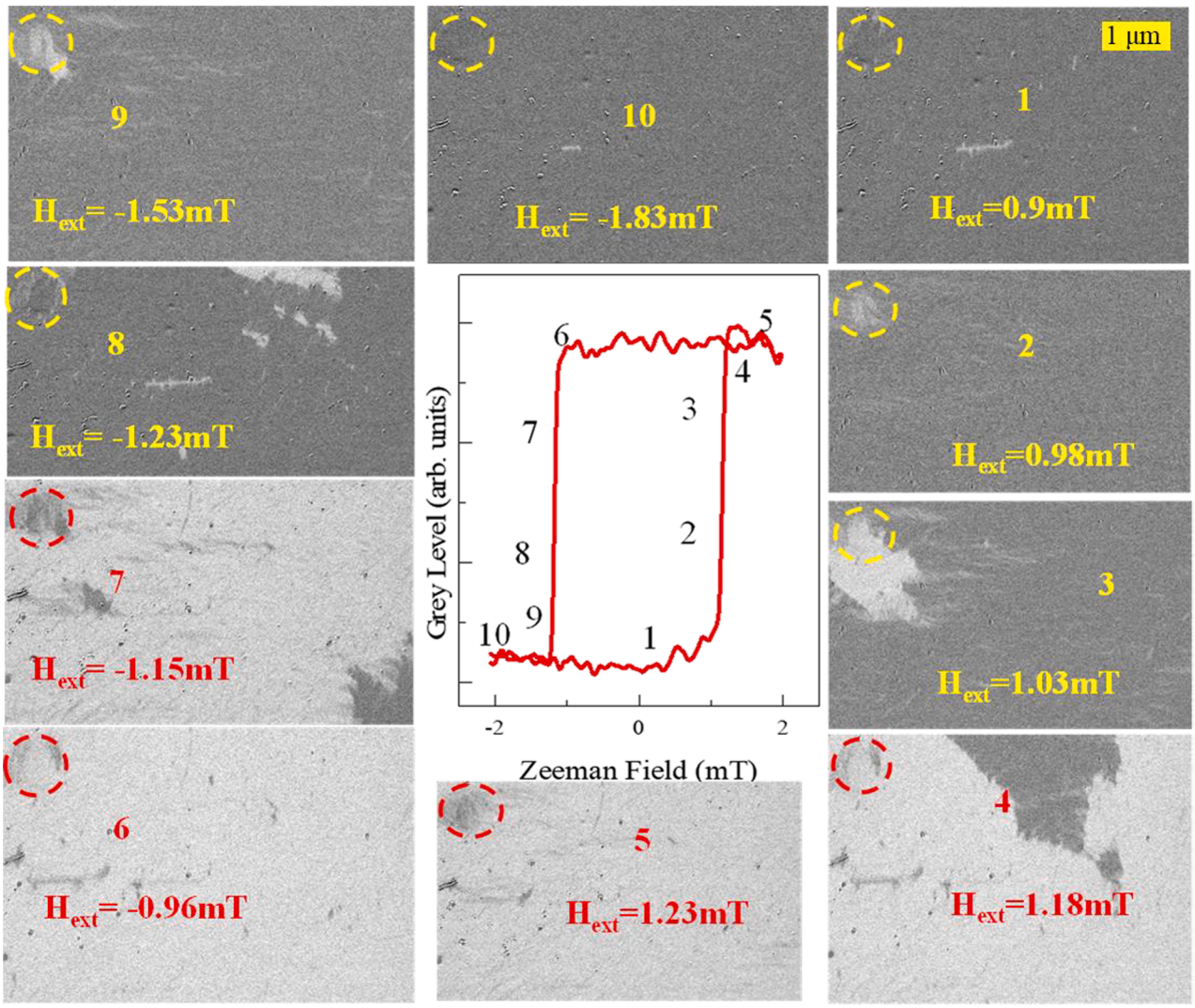

Fig. 4. Longitudinal MOKE hysteresis loop of Fe_2CoGe thin films. (1 – 10) shows MOKE domain images at designated points shown on hysteresis loop. (1–5) shows distorted vortex state with positive applied field and (6–10) vortex state in negative field.

structure that prevails in our films, we performed (a) First order reversal curves (FORC) (b) Magneto-optic Kerr effect (MOKE) (c) Magnetic force microscopy (MFM) and (d) Micromagnetic simulations.

Here we discuss about our results pertinent to FORC measurements. Effect of defects on the domain wall motion has been demonstrated by analysing the data pertinent to FORC [21,25,26]. In our work, initially a single FORC loop is measured by saturating the film along positive saturation magnetization $B_{sat} = 18$ mT. Subsequently, the magnetization (M) is measured using a reversal field (B_a) and saturated back again with steps (B_b) [9,10,24,25]. Indeed, this method is repeated for several values of Ba with step of 0.05mT in the field range of – 20 mT to 20 mT as shown in Fig. 2 (a). Upon closer observation, it is evident from Fig. 2 (a) that there exists a switching field distribution for FORC curve, which is circled. Earlier, spread for the switching field distribution has been evidenced and explained on the basis of domain wall pinning in poly-crystalline Fe, FeGa and Fe_2NiGe thin films respectively [10,26,28]. The magnetization depicted in Fig. 2 (a) can be defined as a polynomial $M(B_a,B_b) = a_1 + a_2B_a + a_3B_a^2 + a_4B_b + a_5B_b^2 + a_6\, B_a\, B_b$ with the use of a smoothing factor (SF) to remove the noise generated during the experiment [27]. Over here, the FORC distribution (ρ) is obtained from a mixed 2nd order derivative of magnetisation surface as [28–30].

$$\rho\,(B_a, B_b) = -\frac{1}{2}\frac{\partial^2 M(B_a,B_b)}{\partial B_a \partial B_b} \quad \ldots\ldots\ldots\ldots\ldots\ldots (1).$$

A Preisach model is used to convert FORC distribution (ρ) in Eq-(1) to FORC diagram [28,31]. According to this model, B_c (local coercivity) $=(B_b - B_a)/2$ and B_u (interaction field) $= (B_b + B_a)/2$ along × and y-axis are obtained by converting the coordinates of FORC distribution (B_a, B_b) [10,28]. Fig. 2 (b) depicts the contour graph between B_c vs B_u, that demonstrates the presence of the positive–negative ridges on B_u axis. The small negative features with blue colour in the FORC diagrams near (B_u, B_c) = (- 2 mT, 0 mT) & (- 3 mT, 5 mT) are due to numerical artefacts [33]. The other feature in Fig. 2 (b) are not related to the numerical artifacts [10,26,28,32]. The presence of contour graphs in B_c vs B_u has been attributed to mean-field that exists inside the thin film. Indeed, this confirms the presence of the switching fields distribution[9]. Over here, the mean field depends on the demagnetization factor and has been demonstrated due to the effect of the local field experienced by the hysteron in the external magnetic field [9,28].Yet in another study, C. Grech *"et al."* have shown the creation of the positive valued FORC "ridge" and negative valued FORC "edge" in the array of nanomagnet system [23]. From the Fig. 2(b) it is clear that there exists a central dark region which is due to the reversal of magnetization at the switching field [9,28]. From the spread of central dark region, we infer that there exists distribution for the switching fields with a coercivity distribution ~ 2 mT.

FORC analysis has been used to determine the magnetostatic interaction(MI) strength between magnetic grains through switching field

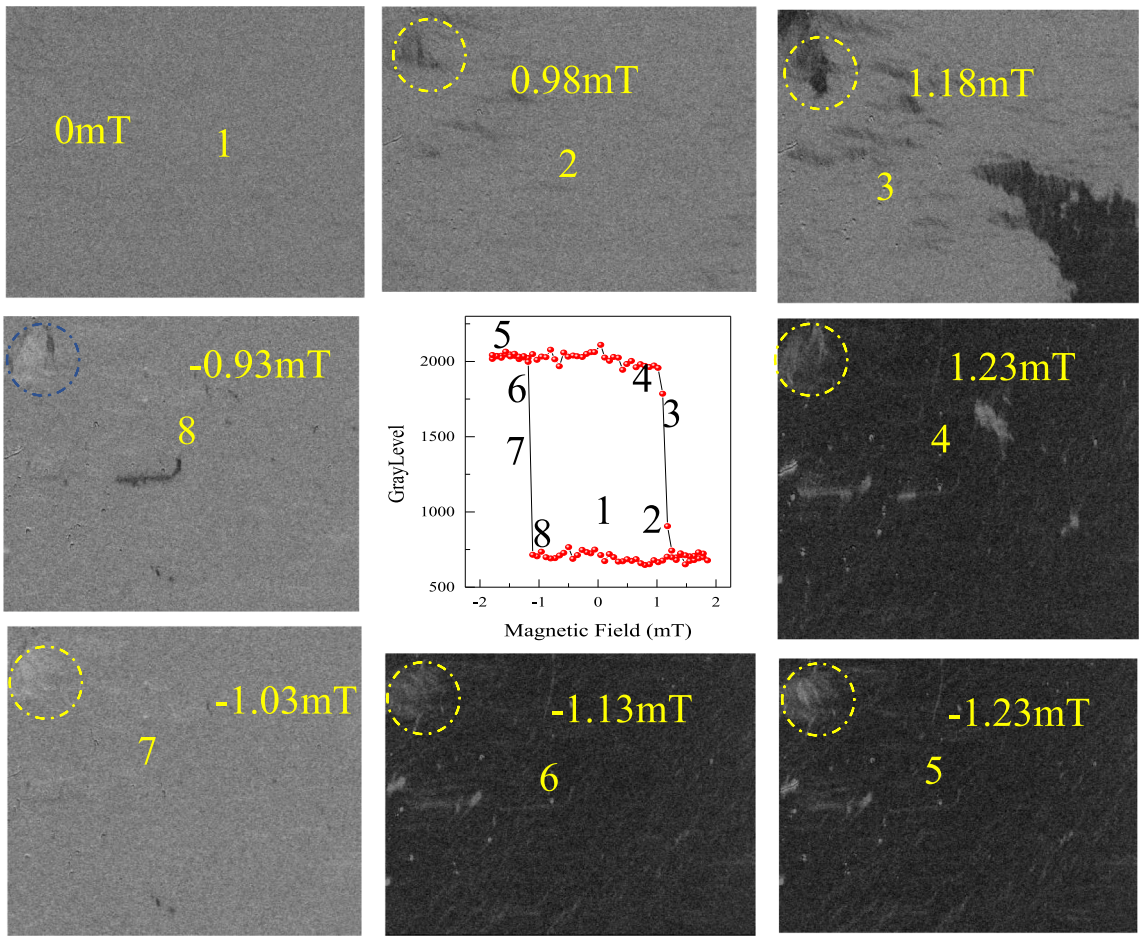

Fig. 5. Hysteresis loop at room temperature using magneto optical Kerr effect (MOKE) along hard axis (210°) of Fe_2CoGe thin films. (1 – 8) MOKE domain images at designated points shown on hysteresis loop.

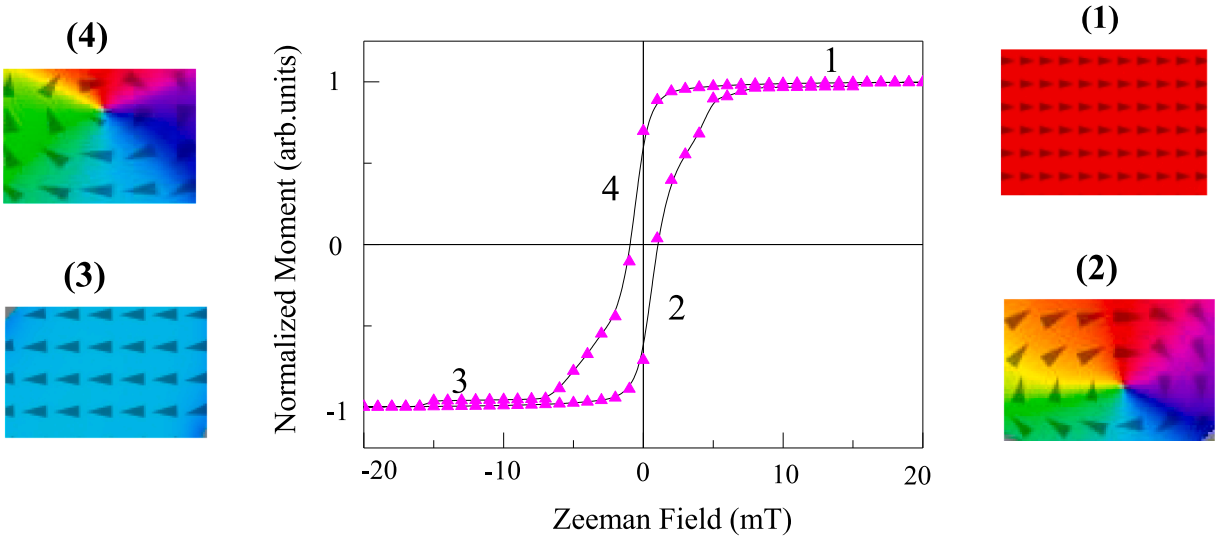

Fig. 6. Simulated hysteresis loop for Fe_2CoGe thin films where (1), (3) represent single domain state (SD) and (2), (4) denote vortex state (VS).

distribution (SFD) [35–37]. In general, the SFD is defined as (δ M (B_a, B_b) / δ B_a), which is obtained by taking the first derivative of M (B_a, B_b) at each of the magnetization reversal point with respect to the B_a, which is depicted in Fig. 2 (c) for Fe_2CoGe thin film. Full width at half maxima (FWHM) that demonstrates the MI is determined from SFD vs B_a graph and is found to be 7.54 mT. Earlier, dipolar field has been calculated on Fe nanodots, which is comparable with the present FWHM [28]. Fig. 2 (d) shows the 3D view of FORC distribution, which explains the formation of vortex state (VS) in our thin film [6,27,34,35].

To get more insights and to confirm on the vortex state that is evidenced through FORC data, we performed MFM measurements. While doing the experiment we recorded the phase images. Fig. 3 (a) infers

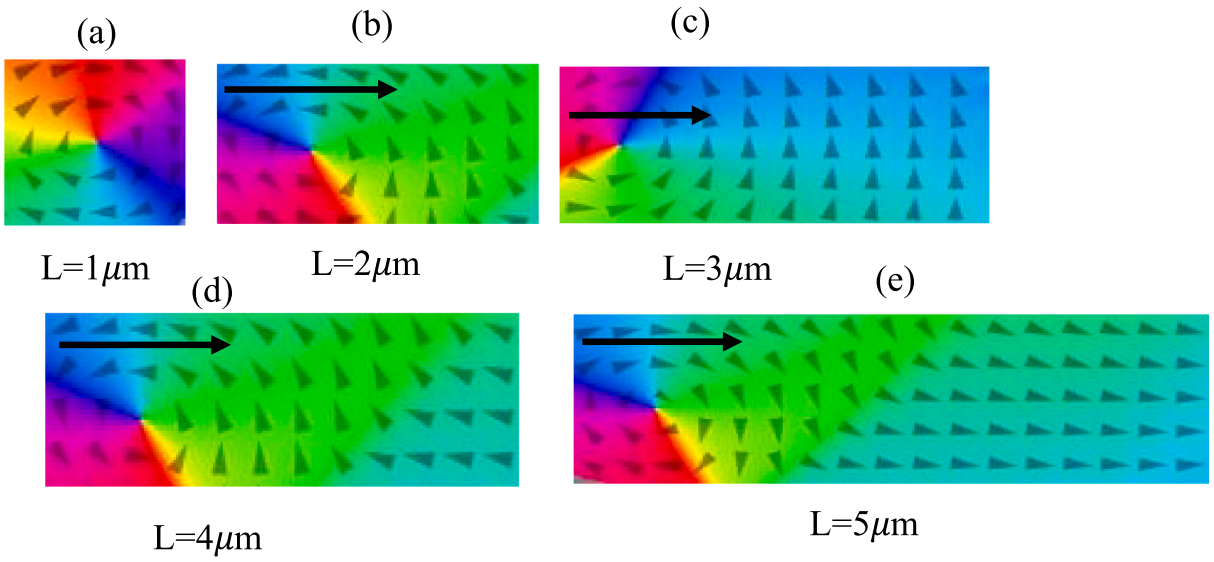

Fig. 7. Formation of vortex state in (a) square and (b,c,d,e) rectangle with length 2 μm,3 μm, 4 μm and 5 μm respectively in Fe_2CoGe thin film.

AFM image of the Fe_2CoGe thin film, which indicates the surface is rather smooth with a roughness ~ 1.26 nm. Fig. 3 (b - i) depicts the schematic of the magnetic tip that we used to extract MFM phase image with a lift height of 80 nm. The tip was magnetized with 10 mT field with an angle of 35° before we performed the measurements. Over here, the phase shift of cantilever oscillations under the gradient of a magnetic field was registered as the MFM contrast. It is clear from the Fig. 3(b - ii) that the Fe_2CoGe thin film consists of in-plane magnetic domain. Indeed, there exists a dark region that resembles as though there exists vortex state in the Fe_2CoGe thin film. Here the dark and yellow colour contrast signifies different magnetic domains. Interestingly, realization of VS through MFM matches with the earlier reports [12,13]. Sina Mayr *"et al."* have reported magnetic vortex state in Co/ $Ru/Ni_{81}Fe_{19}$ trilayer system through MFM phase imaging [36]. M. Natali *"et al."* have reported VS formation in Co dot arrays [39]. Hence, we believe that the features that we observed in the MFM phase image is evidence for the formation of the vortex state, which is consistent with the FORC data analysis.

To further elucidate the existence of vortex state, microscopic magnetic behaviour, magnetic domain structures and the spatial distribution of magnetic moment orientation we performed the magneto-optic Kerr effect (MOKE). In general, MOKE measurements can be done in three different optical and magnetic geometries, (a) Polar MOKE (b) Longitudinal MOKE (L – MOKE) and (c) Transverse MOKE [40]. MFM study suggests the formation of VS when the tip is magnetized in the homogeneous magnetic field at an inclined angle ~ 30°. Motivated from the above experiment, we performed L-MOKE measurements when the angle between magnetic field and film edge is 30° and 210° respectively and are shown in Fig. 4 and Fig. 5. To realize the existence of VS from L – MOKE, we also tried to image the magnetic domains at different regions during the magnetization reversal as shown in Fig. 4 and Fig. 5. We confirm the existence of VS through MOKE images as follows. When the angle between film edge and magnetic field is 30°, we do see the formation of vortex state i.e., more specifically the contrast of domain image is dark in the circled region in Fig. 4 (4–7). Again, if we see the image for 210° angle between film edge and magnetic field in the same region the contrast colour changes to white as shown in Fig. 5 (4–7). Interestingly, similar kind of behaviour has been observed by M. Natali, "*et al.*" in Co-nanodot [39].The vortex nucleation and annihilation mechanism has been mainly investigated for widely spaced dots and multilayer thin film, both theoretically and experimentally [38,40–43]. Interestingly with negative magnetic field as well, we do see feature for the VS in the circled region. This suggest that VS is conserved its chirality irrespective of applied field direction[14,15].

We also performed micromagnetic simulations on the thin films of Fe_2CoGe using $MuMax^3$ software [42] which solves the Landau–Lifshitz–Gilbert (LLG) equation which is given below.

$$\frac{\partial M}{\partial t} = -\gamma_0 M \times H_{eff} - \alpha M \times \frac{\partial M}{\partial t} \quad (2)$$

where γ_0 is the gyromagnetic ratio, H_{eff} is the effective magnetic field and cubic cell size (mesh size) of 5 nm × 5 nm × 5 nm is used for the simulations. Over here we used the film size of 1500 nm (L) × 1000 nm (w) × 110 nm (t), ferromagnetic exchange stiffness constant (A) ~ 60 pJ/m [43–45], and $K_u = 1.74 \times 10^4$ J/m^3.The cell size is chosen to be slightly smaller than the exchange length, which is estimated using the equation $l_{ex} = \frac{\sqrt{2A/\mu_0}}{M_S}$ [46] and is found to be 5.85 nm. Simulated M−H loop and corresponding domain images are shown in Fig. 6. We do see the formation of vortex state in Fe_2CoGe thin films before the saturation or near the transition region as shown in the domain images 2 & 4. The size of vortex is ~ 1 μm. Z. M. Dai, "*et al.*" have shown the nucleation of vortex state in the $[Co/Pd]_7/Ru/Py$ multilayer structure[15]. In a similar study, M. Natali "*et al.*" has proved the existance of VS in Cobalt dot arrays using micromagnetic simulation [39]. In order to check the stability of VS texture in Fe_2CoGe thin film we have performed simulation with different shape and size of the Fe_2CoGe structures as shown in Fig. 7. Over here, we varied the length of film from 1–5 μm. We do not observe any increase in vortex size (~1 μm) irrespective of change in length of structure. From the above analysis we can say the VS in Fe_2CoGe thin film is an isolated texture. Indeed, the existence of VS is correlated with our other measurements such as FORC, MOKE, and MFM respectively.

In summary, we performed detailed experimentation and simulations to realize vortex state in Fe_2CoGe thin films. In particular, vortex state using FORC confirmed from contour graph that is obtained through the switching field distribution. The results pertinent to MFM suggests vortex state with the dark regions, which are characterized by the curling of magnetization with in the in-plane direction. The existence of dark region irrespective of change in the magnetic field direction confirms the vortex state through L-MOKE images. Above results are supported by the domain image obtain by MUMAX3 simulations using LLG equation. We believe that present results will be helpful for the utilization of Fe_2CoGe thin films for the future spintronic applications.

Declaration of Competing Interest

The authors declare that they have no known competing financial interests or personal relationships that could have appeared to influence the work reported in this paper.

Data availability

Data will be made available on request.

Acknowledgements

We would like to thank Indian Institute of Technology Hyderabad (IITH) for financial assistance. SNJ would like to thank DST – SERB Core research grant (CRG/2020/003497) and DST – FIST for the grant (SR/FST/PSI-215/2016). Rajesh Kumar Roul would like to thank DST – Inspire for the fellowship.

References

[1] G. Dai, X. Xing, W. Yan, Y. Shen, X. Deng, J. Appl. Phys. 132 (2022), 043901.
[2] H. Vigo-Cotrina, A.P. Guimarães, J. Magn. Magn. Mater. 460 (2018) 160.
[3] J.T.S. Dantas, R.M. Souza, A.S. Carriço, S.M.S.B. Martins, L.L. Oliveira, A.L. Dantas, J. Appl. Phys. 131 (2022), 093901.
[4] R.K. Gupta, S.R. Mishra, and T.A. Nguyen, editors , *Emerging Applications of Low Dimensional Magnets*, First edition (CRC Press, Boca Raton, FL, 2023)).
[5] B. Pigeau, G. de Loubens, O. Klein, A. Riegler, F. Lochner, G. Schmidt, L. W. Molenkamp, Nature Phys 7 (2011) 26.
[6] M.A. Valdez-Grijalva, A.R. Muxworthy, W. Williams, P.Ó. Conbhuí, L. Nagy, A. P. Roberts, D. Heslop, Earth Planet. Sci. Lett. 501 (2018) 103.
[7] C.C.I. Ang, W. Gan, G.D.H. Wong, W.S. Lew, Phys. Rev. B 103 (2021), 144409.
[8] N.K. Duong, R. Tomasello, M. Raju, A.P. Petrović, S. Chiappini, G. Finocchio, C. Panagopoulos, APL Mater. 8 (2020), 111112.
[9] G.T. Zimanyi and M. Winklhofer, in *2009 International Conference on Electromagnetics in Advanced Applications* (IEEE, Torino, Italy, 2009), pp. 979–982.
[10] A. Stancu, C. Pike, L. Stoleriu, P. Postolache, D. Cimpoesu, J. Appl. Phys. 93 (2003) 6620.
[11] C. Pike, A. Fernandez, J. Appl. Phys. 85 (1999) 6668.
[12] I. Lascu, J.F. Einsle, M.R. Ball, R.J. Harrison, J. Geophys. Res. Solid Earth 123 (2018) 7285.
[13] E. Pinilla-Cienfuegos, S. Mañas-Valero, A. Forment-Aliaga, E. Coronado, ACS Nano 10 (2016) 1764.
[14] J. Chang, V.L. Mironov, B.A. Gribkov, A.A. Fraerman, S.A. Gusev, S.N. Vdovichev, J. Appl. Phys. 100 (2006), 104304.
[15] Z.M. Dai, Y.Y. Dai, W. Liu, T.T. Wang, X.T. Zhao, X.G. Zhao, Z.D. Zhang, Appl. Phys. Lett. 111 (2017), 022404.
[16] P. Vavassori, N. Zaluzec, V. Metlushko, V. Novosad, B. Ilic, M. Grimsditch, Phys. Rev. B 69 (2004), 214404.
[17] S. Gupta, Z.R. Tadisina, A.L. Highsmith, X. Li, C.L. Guenther, B.D. Clark, Y. Inaba, G.B. Thompson, W. Xu, P.R. LeClair, *Mater. Res. Soc. Symp. Proc.* (Materials Research Society (2008).
[18] A. Hirohata, W. Frost, M. Samiepour, J. Kim, Materials 11 (2018) 105.
[19] T. Gasi, V. Ksenofontov, J. Kiss, S. Chadov, A.K. Nayak, M. Nicklas, J. Winterlik, M. Schwall, P. Klaer, P. Adler, C. Felser, Phys. Rev. B 87 (2013), 064411.
[20] Z. Ren, S.T. Li, H.Z. Luo, Phys. B Condens. Matter 405 (2010) 2840.
[21] G.W. Brindley, Philos. Mag. 36 (1945) 347–369.
[22] https://www.azom.com/article.aspx?ArticleID=20003.
[23] H.M. Rietveld, J Appl Crystallogr 2 (1969) 65.
[24] D.P. Rai, Lalrinkima, Lalhriatzuala, L.A. Fomin, I.V. Malikov, A. Sayede, M.P. Ghimire, R.K. Thapa, and L. Zadeng, RSC Adv. **10**, 44633 (2020).
[25] A. Seeger, H. Kronmüller, H. Rieger, H. Träuble, J. Appl. Phys. 35 (1964) 740.
[26] B.B. Nayak, S.N. Jammalamadaka, J. Magn. Magn. Mater. 536 (2021), 168107.
[27] R. Kumar Roul, A. Kumar Jana, B.B. Nayak, S. Narayana Jammalamadaka, J. Magn. Magn. Mater. 556 (2022), 169401.
[28] C. Grech, M. Buzio, M. Pentella, N. Sammut, Materials 13 (2020) 2561.
[29] D. Heslop, A.R. Muxworthy, J. Magn. Magn. Mater. 288 (2005) 155.
[30] R.K. Dumas, C.-P. Li, I.V. Roshchin, I.K. Schuller, K. Liu, Phys. Rev. B 75 (2007), 134405.
[31] F. Béron, D. Ménard, A. Yelon, J. Appl. Phys. 103 (2008) 07D908.
[32] J.E. Davies, O. Hellwig, E.E. Fullerton, K. Liu, Phys. Rev. B 77 (2008), 014421.
[33] D.A. Gilbert, G.T. Zimanyi, R.K. Dumas, M. Winklhofer, A. Gomez, N. Eibagi, J. L. Vicent, K. Liu, Sci Rep 4 (2015) 4204.
[34] C.R. Rementer, K. Fitzell, Q. Xu, P. Nordeen, G.P. Carman, Y.E. Wang, J.P. Chang, Appl. Phys. Lett. 110 (2017), 242403.
[35] A.K. Jana, M.M. Raja, J.A. Chelvane, S.N. Jammalamadaka, IEEE Trans. Magn. 58 (2022) 1.
[36] A. Muxworthy, W. Williams, J. Appl. Phys. 97 (2005), 063905.
[37] D.R. Cornejo, T.R.F. Peixoto, S. Reboh, P.F.P. Fichtner, V.C. de Franco, V. Villas-Boas, F.P. Missell, J Mater Sci 45 (2010) 5077.
[38] S. Mayr, L. Flajšman, S. Finizio, A. Hrabec, M. Weigand, J. Förster, H. Stoll, L. J. Heyderman, M. Urbánek, S. Wintz, J. Raabe, Nano Lett. 21 (2021) 1584.
[39] M. Natali, I.L. Prejbeanu, A. Lebib, L.D. Buda, K. Ounadjela, Y. Chen, Phys. Rev. Lett. 88 (2002), 157203.
[40] A. Hubert and R. Schäfer, *Magnetic Domains: The Analysis of Magnetic Microstructures*, Corr. print., [Nachdr.] (Springer, Berlin, 2011).
[41] R.P. Cowburn, D.K. Koltsov, A.O. Adeyeye, M.E. Welland, D.M. Tricker, Phys. Rev. Lett. 83 (1999) 1042.
[42] A. Lebib, S.P. Li, M. Natali, Y. Chen, J. Appl. Phys. 89 (2001) 3892.
[43] A. Fernandez, C.J. Cerjan, J. Appl. Phys. 87 (2000) 1395.
[44] A. Vansteenkiste, J. Leliaert, M. Dvornik, M. Helsen, F. Garcia-Sanchez, B. Van Waeyenberge, AIP Adv. 4 (2014), 107133.
[45] V. Asvini, G. Saravanan, R.K. Kalaiezhily, M.M. Raja, and K. Ravichandran, in (Mumbai, India, 2018), p. 130051.
[46] G.S. Abo, Y.-K. Hong, J. Park, J. Lee, W. Lee, B.-C. Choi, IEEE Trans. Magn. 49 (2013) 4937.